Clim Dyn (2013) 40:1671–1686
DOI 10.1007/s00382-012-1495-9

An estimate of equilibrium sensitivity of global terrestrial carbon cycle using NCAR CCSM4

G. Bala · Sujith Krishna · Devaraju Narayanappa · Long Cao · Ken Caldeira · Ramakrishna Nemani

Received: 10 January 2012 / Accepted: 11 August 2012 / Published online: 26 August 2012

Abstract Increasing concentrations of atmospheric CO_2 influence climate, terrestrial biosphere productivity and ecosystem carbon storage through its radiative, physiological and fertilization effects. In this paper, we quantify these effects for a doubling of CO_2 using a low resolution configuration of the coupled model NCAR CCSM4. In contrast to previous coupled climate-carbon modeling studies, we focus on the near-equilibrium response of the terrestrial carbon cycle. For a doubling of CO_2, the radiative effect on the physical climate system causes global mean surface air temperature to increase by 2.14 K, whereas the physiological and fertilization on the land biosphere effects cause a warming of 0.22 K, suggesting that these later effects increase global warming by about 10 % as found in many recent studies. The CO_2-fertilization leads to total ecosystem carbon gain of 371 Gt-C (28 %) while the radiative effect causes a loss of 131 Gt-C (~10 %) indicating that climate warming damps the fertilization-induced carbon uptake over land. Our model-based estimate for the maximum potential terrestrial carbon uptake resulting from a doubling of atmospheric CO_2 concentration (285–570 ppm) is only 242 Gt-C. This highlights the limited storage capacity of the terrestrial carbon reservoir. We also find that the terrestrial carbon storage sensitivity to changes in CO_2 and temperature have been estimated to be lower in previous transient simulations because of lags in the climate-carbon system. Our model simulations indicate that the time scale of terrestrial carbon cycle response is greater than 500 years for CO_2-fertilization and about 200 years for temperature perturbations. We also find that dynamic changes in vegetation amplify the terrestrial carbon storage sensitivity relative to a static vegetation case: because of changes in tree cover, changes in total ecosystem carbon for CO_2-direct and climate effects are amplified by 88 and 72 %, respectively, in simulations with dynamic vegetation when compared to static vegetation simulations.

Keywords Climate change · Terrestrial carbon cycle · CO_2-physiological effect · CO_2-fertilization · Carbon cycle feedback

Electronic supplementary material The online version of this article (doi:10.1007/s00382-012-1495-9) contains supplementary material, which is available to authorized users.

G. Bala (✉) · S. Krishna · D. Narayanappa
Divecha Center for Climate Change, Center for Atmospheric and Oceanic Sciences, Indian Institute of Science, Bangalore 560012, India
e-mail: bala.gov@gmail.com; gbala@caos.iisc.ernet.in

L. Cao
Department of Earth Sciences, Zhejiang University, Hangzhou 310027, Zhejiang Province, China

K. Caldeira
Department of Global Ecology, Carnegie Institution, 260 Panama Street, Stanford, CA 94305, USA

R. Nemani
NASA Ames Research Center, Moffett Field, CA 94035, USA

1 Introduction

Rapidly increasing atmospheric CO_2 concentration since the preindustrial period is caused mainly by anthropogenic sources of CO_2 from fossil fuel emissions and land cover change. In the most recent decade (2000–2009), about 90 % of anthropogenic CO_2 emissions are from fossil fuel burning and cement production and the rest due to land cover change (Le Quere et al. 2009). Accumulation of CO_2 in the atmosphere is critically dependent on the capacity of

oceanic and terrestrial sinks and the rate of emissions (Schimel et al. 1995). Slightly less than half of present day anthropogenic CO_2 emission accumulates in the atmosphere and the rest is taken up by land and oceans (House et al. 2003; Le Quere et al. 2009; Prentice et al. 2001).

The terrestrial carbon cycle plays an important role in determining the fraction of anthropogenic CO_2 that stays in the atmosphere via uptake through photosynthesis and release through respiration. Increasing atmospheric CO_2 concentration allows plants to increase the amount of CO_2 uptake per molecule of water lost through the leaves. This leads both to reduced loss of water and increased uptake of CO_2. The stimulation of vegetation productivity in the absence of other limiting factors is known as CO_2-fertilization (Curtis 1996; Owensby et al. 1999; Prentice et al. 2001). Experimental studies provide evidence for CO_2-fertilization: for example, free-air CO_2 enrichment experiments in forest (Norby et al. 2005) indicated $\sim$23 % median increase in net primary production (NPP) when CO_2 is increased from 376–550 ppm. CO_2-fertilization results in negative climate feedback, i.e. it suppresses CO_2 accumulation in atmosphere due to increased land biosphere uptake. In contrast, warming-induced increases in heterotrophic or soil respiration (Govindasamy et al. 2005; Lloyd and Taylor 1994; Matthews et al. 2005; Thompson et al. 2004; Zeng et al. 2004) tend to accelerate global warming by diminishing or even reversing the net CO_2 flux from the atmosphere to the land biosphere (Cox et al. 2000; Cramer et al. 2001; Friedlingstein et al. 2001; Joos et al. 1991). In some of the models, terrestrial ecosystem remains a net sink of CO_2 throughout the twenty-first century or longer (Bala et al. 2005; Friedlingstein et al. 2006), but in others the land biosphere becomes a net source of CO_2 by the middle of twenty-first century (Betts et al. 2004; Cox et al. 2000).

CO_2-fertilization is one of the most important determinants of the rate of CO_2 accumulation in the atmosphere over the next century. The current generations of coupled climate-carbon models show increases in terrestrial carbon uptake as a result of CO_2-fertilization. Long-term tree ring studies suggest a more complex picture and perhaps a lack of universality of the CO_2 fertilization effect, albeit these studies have their own difficulties in separating other variables such as temperature and the availability of water and nutrients, which interact with the CO_2 fertilization response (Gedalof and Berg 2010). The extent to which CO_2 fertilization is responsible for current terrestrial carbon uptake, as well as potential for this process to further stimulate the future terrestrial carbon uptake, is not clear and is currently the focus of a large body of active research.

In this paper, our main goal is to estimate the maximum potential carbon sink over land using a comprehensive state of the art coupled climate and carbon cycle model. This potential carbon uptake is dominated by two important factors as discussed above: climate change and the CO_2-fertilization effects. This study mainly aims to estimate the equilibrium uptakes from these two factors using multi-century simulations for an idealized scenario (instantaneous doubling atmospheric CO_2 with no dynamic change in vegetation). This bounding exercise in this study reveals the limited storage capacity of the terrestrial biosphere. In addition, previous modeling studies suggest that because of lags in the terrestrial ecosystem response, long term changes to terrestrial carbon cycle should be considered in the definition of dangerous climate change and policy development aimed at avoiding it (Jones et al. 2009).

We have used the NCAR CCSM4 climate model. Since our goal is the estimation of the maximum potential land biosphere uptake, we run the coupled model to a near-equilibrium state for a doubling of atmospheric CO_2. In the past, only a few studies have investigated the equilibrium response of the terrestrial biosphere using comprehensive global models. Good et al. (2011) investigated the equilibrium response of tropical forest to climate and CO_2 using the Hadley Center coupled climate and carbon cycle model. Using the same model Jones et al. (2009, 2010) investigated the long-term response of the terrestrial ecosystems. They find that the biosphere continues to respond even after climate stabilization for decades or even centuries following emissions reductions. They further show that the processes of forest dieback are hard to diagnose in transient climate projections because of the substantial lag in forest response to climate changes (Jones et al. 2009).

Here, the *CO_2-radiative effect* refers to the climate and carbon cycle consequences of CO_2 changes in the atmosphere that derive from the radiative properties of CO_2. The *CO_2-physiological effect* refers to the climate and carbon cycle consequences of reduced opening of stomata in leaves resulting from elevated CO_2-concentrations and the consequent reduction in surface latent heat fluxes, and the *CO_2-fertilization effect* refers to the climate and carbon cycle consequences of stimulated photosynthesis and the associated increases in leaf area index (LAI), net primary productivity (NPP), and carbon stocks in leaves, stems and roots. The climate response due to this later effect has been also referred as *structural vegetation change effect* in an earlier study (Betts et al. 1997). We use the term "*CO_2-direct effect*" (Cox et al. 1999; Gedney et al. 2006) to refer to the climate-carbon response when both CO_2-physiological and CO_2-fertilization effects are taken together into consideration. Lastly, the term "*combined effects*" refers to the combination of CO_2-radiative, CO_2-physiological and CO_2-fertilization effects (i.e., to the combination of CO_2-radiative and CO_2-direct effects).

In the next two sections, we describe the model used and experimental setup. In the following section, we quantify the equilibrium climate and terrestrial carbon cycle changes for a doubling of CO_2 concentration in the atmosphere with respect

to preindustrial times. We also make an estimate of carbon storage sensitivities to temperature and atmospheric CO_2 concentration in this section and compare them with previous modeling studies. Conclusions are presented in the last section.

2 Model

The model used for this study is the NCAR (National Center for Atmospheric Research) Community Climate System Model version 4 (CCSM 4). A general overview of CCSM4 and its performance relative to CCSM3 is provided in (Gent et al. 2011). CCSM4 is a coupled global climate model consisting of atmosphere, land, ocean and sea-ice components that are linked through a coupler that exchanges state information and fluxes between the components. The atmospheric component of CCSM4 is the Community Atmosphere Model version 4 (CAM4). CAM4 uses 26 layers in vertical. The Parallel Ocean Program version 2 (POP2) is the ocean component in CCSM4 which has a total of 60 levels in the vertical with 10 m vertical resolution in the upper 200 m. There is no ocean carbon cycle component in the configuration of CCSM4 adopted for this study. The CCSM4 sea ice component is the Community Ice Code version 4 and the land component of CCSM4 is the Community Land Model version 4 (CLM4) (Lawrence et al. 2011; Oleson et al. 2010).

The land component CLM4 succeeds CLM3.5 with revised hydrology and snow models, organic soils, and a 50 m deep ground column (Bonan and Levis 2010). CLM4 includes carbon–nitrogen biogeochemistry with prognostic carbon and nitrogen in vegetation, litter, and soil organic matter (Randerson et al. 2009; Thornton et al. 2009; Thornton et al. 2007). Vegetation is represented by leaf, fine root, respiring and non-respiring stem and coarse root, and storage pools. Leaf phenology is simulated for evergreen, seasonal deciduous and stress-deciduous plants. The heterotrophic model represents coarse woody debris, three litter pools, and four soil organic matter pools. A prognostic fire model simulates wildfire (Kloster et al. 2010). CLM4 does retain the dynamic vegetation biogeography (competition) aspects of the CLM3 dynamic vegetation module DGVM (Levis et al. 2004). However, for the simulations in this study, we do not exercise the DGVM option except in Sect. 4.3 where we briefly discuss the sensitivity of the total ecosystem carbon changes to dynamic vegetation in off-line simulations.

3 Experiments

We use the low resolution version T31 of CCSM4 for our experiments. The horizontal resolution in the atmosphere model is approximately 3.75° and it is about 3° for the ocean model. All our simulations start from a well spun up preindustrial state of the model climate which was provided by NCAR (Christine Shields, Personal communication). Four 500-year CCSM4 simulations were performed: (1) a control simulation "1 × CO_2" in which the model is forced with the preindustrial CO_2 level (285 ppm); (2) a doubled CO_2 simulation "2 × CO_2" in which both CAM4 and CLM4 are forced by CO_2 concentration of 570 ppm. This experiment simulates the radiative as well as CO_2-physiological and CO_2-fertilization effects of increased CO_2. (3) "RAD" in which a CO_2 concentration of 570 ppm is prescribed to CAM4 but CLM4 is forced by 285 ppm. In this simulation, only the radiative effect of CO_2 is simulated; (4) "BGC" where we isolate CO_2-direct effect by forcing only CLM4 with 570 ppm. It should be noted that we do not attempt to separate the CO_2-direct effect into the physiological and fertilization effects in this study. Carbon–nitrogen dynamics is included in the land model but nitrogen deposition is kept constant at preindustrial levels in all the simulations. Land cover change is not included in the model. Evolution of various global- and annual-mean variables in the atmosphere and land-biosphere in the last 100-years are plotted in Fig. S1 which shows that the simulations have reached near-equilibrium conditions by 400 years. Specifically, net radiative flux at top of the atmosphere (Fig. S1f) and net ecosystem exchange (NEE) have stabilized (Fig. S1k) by this time. We use the last 100 years of simulations for the analysis. During this 100 year period, TOA net flux is -0.049 Wm^{-2} and NEE is 0.1 Gt-C per year for the 1 × CO_2 case. The drift in global mean surface temperature is $\sim 0.05 \pm 0.004$ K per century and soil carbon drift is -0.0367 ± 0.0001 Gt-C per year which shows that the model has attained a near-equilibrium state.

4 Results and discussions

4.1 Response of climate and land-biosphere parameters

In this section, we present the results of radiative effect (RAD-1 × CO_2), CO_2-direct effect (BGC-1 × CO_2) and the combined effect (2 × CO_2 − 1 × CO_2). For a doubling of CO_2, Fig. 1 shows the simulated response of 24 important parameters, such as temperature, precipitation, gross primary production (GPP), net ecosystem exchange (NEE), evapotranspiration, biomass carbon, soil carbon etc., resulting from the radiative effect, CO_2-direct effect and combined effect in the last 100 years. Table 1 lists these changes and percentage changes (in some cases) relative to preindustrial case (1 × CO_2).

The global mean surface air warms by (see Table 1) 2.14 ± 0.02 K due to radiative effect from a doubling of

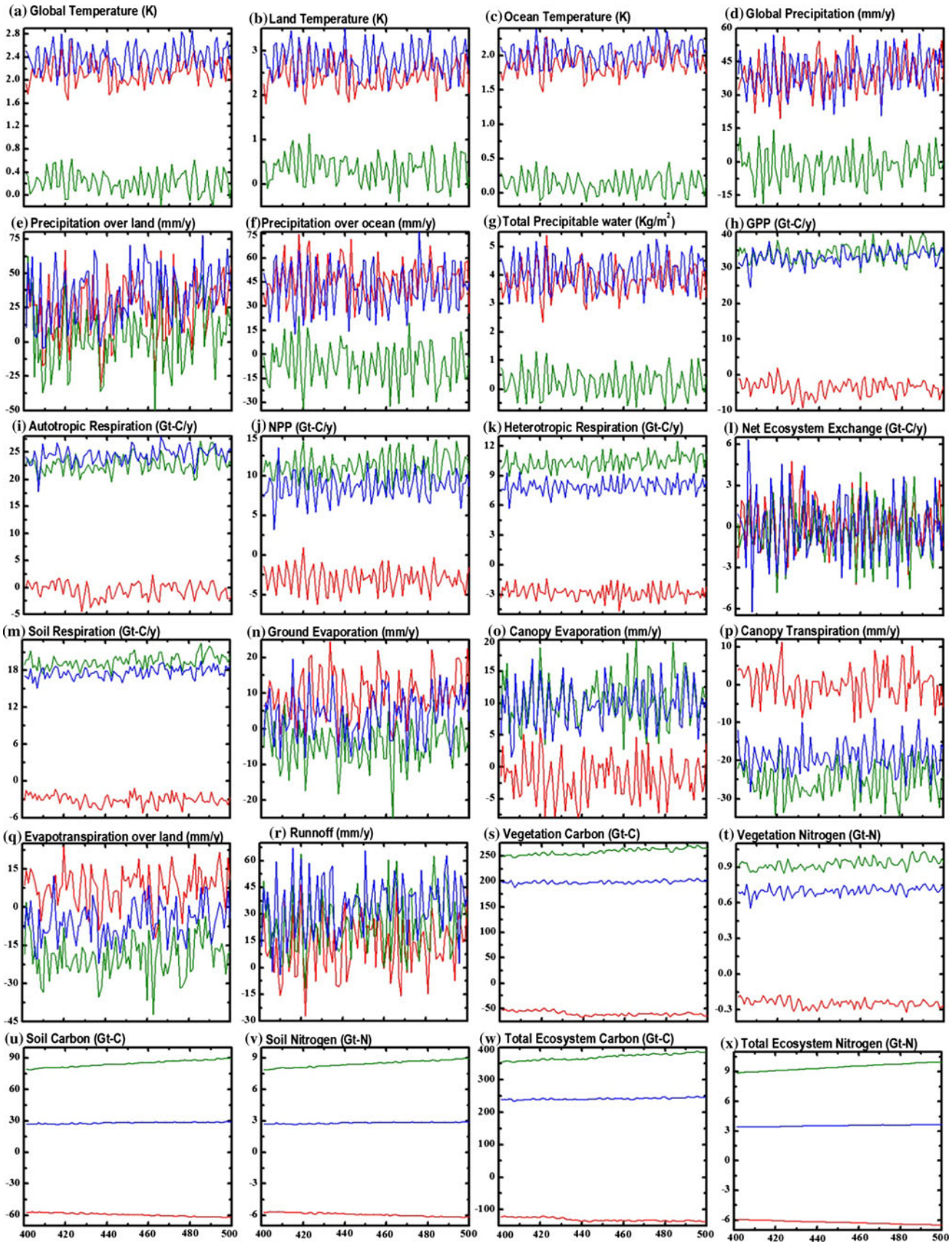
(a) Global Temperature (K)
(b) Land Temperature (K)
(c) Ocean Temperature (K)
(d) Global Precipitation (mm/y)
(e) Precipitation over land (mm/y)
(f) Precipitation over ocean (mm/y)
(g) Total Precipitable water (Kg/m^2)
(h) GPP (Gt-C/y)
(i) Autotropic Respiration (Gt-C/y)
(j) NPP (Gt-C/y)
(k) Heterotropic Respiration (Gt-C/y)
(l) Net Ecosystem Exchange (Gt-C/y)
(m) Soil Respiration (Gt-C/y)
(n) Ground Evaporation (mm/y)
(o) Canopy Evaporation (mm/y)
(p) Canopy Transpiration (mm/y)
(q) Evapotranspiration over land (mm/y)
(r) Runnoff (mm/y)
(s) Vegetation Carbon (Gt-C)
(t) Vegetation Nitrogen (Gt-N)
(u) Soil Carbon (Gt-C)
(v) Soil Nitrogen (Gt-N)
(w) Total Ecosystem Carbon (Gt-C)
(x) Total Ecosystem Nitrogen (Gt-N)
400 420 440 460 480 500

◀ **Fig. 1** Changes in global and annual means of key climate and land-biosphere variables in response to CO_2 radiative effect (RAD-1 × CO_2; *red line*), CO_2-direct effect (BGC-1 × CO_2; *green line*), and combined effect (2 × CO_2 − 1 × CO_2; *blue line*) in the last 100 years

atmospheric CO_2. The mean land surface warming is 2.44 ± 0.04 K and ocean mean warming is 1.88 ± 0.02 K. Average global surface air temperature increases by 0.22 ± 0.02 K in response to CO_2-physiological and CO_2-fertilization effects: physiological effect leads to closure of the stomata, reduced canopy transpiration (Collatz et al. 1992; Sellers et al. 1996) and surface warming (Cao et al. 2010) and fertilization causes more LAI which would tend to increase evapotranspiration and reduce the warming due to physiological effect. Fertilization-induced enhancements in LAI and SAI (stem area index) could also decrease the surface albedo which can lead to warming. The net warming from CO_2-direct effect is in good agreement with a previous study (Cao et al. 2010) which used CLM3.5 to study only CO_2-physiological effect. Even though CLM4 includes changes to LAI while CLM3.5 does not, cancellation of opposing temperature tendencies from increased transpiration and decreased surface albedo caused by enhanced LAI (more LAI would lead to more transpiration and more absorption of solar radiation) is a potential cause for simulating the similar amount of warming.

CO_2-fertilization results in total vegetation carbon increase (Fig. 1s) which corresponds to an increase in LAI and biomass (Table 1). The increase in LAI could potentially contribute to the decrease in surface albedo (Table 1) (which is primarily driven by warming-induced decrease in snow cover) and warm the surface via absorption of solar radiation (Bala et al. 2006; Matthews 2007). Therefore, CO_2 fertilization effect could provide a positive feedback to global warming scenario but increased LAI due to CO_2-fertilization could damp this feedback by increased transpiration. For combined CO_2-radiative and CO_2-direct effect (2 × CO_2 − 1 × CO_2), global mean surface temperature increases by 2.39 ± 0.02 K, mean surface over land warms by 2.79 ± 0.04 K and mean surface over ocean warms by 2.03 ± 0.02 K, suggesting near-linear addition of CO_2-radiative and CO_2-direct effects in the 2 × CO_2 simulation.

Evapotranspiration over land is the sum of canopy evaporation, canopy transpiration and ground evaporation. Evapotranspiration over land in the case RAD (radiative effect) increases by about 7.99 ± 0.95 mm/year (1.3 %) because of increase in ground evaporation (Fig. 1n). In the case of CO_2-direct effect (BGC), the net effect (Fig. 1q) due to less widely opened plant stomata and the resultant decrease in transpiration and increased LAI and the associated increase in transpiration is a reduction in evapotranspiration by 19.31 ± 0.94 mm/year (3.1 %). When both radiative and direct effects are combined, evapotranspiration decreases by 5.54 ± 0.90 mm/year (0.9 %). Therefore, we find that changes to surface hydrology over land are dominated by CO_2-direct effect as found in earlier studies (Betts et al. 2007; Cao et al. 2010). It is also seen in Fig. 1r and Table 1 that total runoff (surface runoff plus drainage) increases by 9.5 % in case of CO_2 direct effect, whereas by only 4.7 % due to climate change.

The global scale photosynthesis over land is known as gross primary production (GPP) which decreases by 3.6 ± 0.28 Gt-C/year (2.6 %) in RAD because of an increase in temperature. There is also an increase in soil evaporation and warming-induced water stress for photosynthesis: we find decreased soil water content in the forested areas in the tropics (figure not shown). However, for CO_2-direct effect, the GPP of terrestrial vegetation increases by 34.03 ± 0.31 Gt-C/year (25 %) because of CO_2-fertilization. We also find a reduction in evapotranspiration and increases in soil water content in this case (Table 1, spatial plot not shown). For the combined effect, GPP increases by 33.05 ± 0.27 Gt-C/year (24.2 %). The net primary production (NPP) is the amount of carbon that is fixed in living vegetation after maintenance and growth respiration by plants or autotrophs (autotrophic respiration, AR). i.e.,

$$\mathrm{NPP} = \mathrm{GPP} - \mathrm{AR} \quad (1)$$

Similar to GPP, NPP of the terrestrial vegetation declines by 3.05 ± 0.14 Gt-C/year (6.5 %) in RAD, increases by 11.21 ± 0.16 Gt-C/year (23.9 %) in BGC and increases by 8.64 ± 0.16 Gt-C/year (18.4 %) in 2 × CO_2. Our global mean increase in NPP per unit increase in CO_2 is lower when compared to Norby et al. (2005) who showed a 23 % median increase in NPP for a CO_2 change from 376 to of 550 ppm.

Figure 2c shows the zonal mean NPP response over the last 100 years of simulations resulting from the CO_2-radiative effect, the CO_2-direct effect, and the combined effects. In response to radiative effect (RAD), NPP decreases (−112 gC/m^2 per year) near equatorial region because of warming. However, the enhancement in NPP of 272 gC/m^2 per year and 228 gC/m^2 per year in response to CO_2-direct effect and combined effect is seen in the southern hemisphere near equatorial region where P–E is maximum (Fig. 2b, 70 mm/year, 201 mm/year at 10°S) i.e., water availability is enhanced.

Figure 1i and Table 1 show that AR declines in the RAD case by 0.54 ± 0.22 Gt-C/year (0.6 %) mainly because of declines in biomass (Fig. 1s). AR increases by 22.85 ± 0.25 Gt-C/year (25.5 %) in BGC and by 24.4 ± 0.21 Gt-C/year (27.3 %) in combined case

Table 1 Global and annual mean changes of key climatic and terrestrial variables averaged over the last 100 years of the 500-year simulations

	Control: $1 \times CO_2$	Radiative effect: RAD-1 $\times CO_2$	Direct CO_2 effect*: BGC-1 $\times CO_2$	Combined effect: $2 \times CO_2 - 1 \times CO_2$	Sum of the effects[†]
Surface air temperature: global (K)	287.40 ± 0.02	2.14 ± 0.02	0.22 ± 0.02	2.39 ± 0.02	2.36 ± 0.04
Surface air temperature: land (K)	281.08 ± 0.02	2.44 ± 0.04	0.34 ± 0.04	2.79 ± 0.04	2.78 ± 0.06
Surface air temperature: ocean (K)	292.61 ± 0.01	1.88 ± 0.02	0.13 ± 0.01	2.03 ± 0.02	2.01 ± 0.03
Total precipitation (mm/year)	1,050.31 ± 0.53	39.40 ± 0.84 (3.8)[a]	−1.80 ± 0.70 (−0.1)	40.60 ± 0.89 (3.8)	37.60 ± 1.31 (3.6)
Total precipitation over land (mm/year)	839.50 ± 0.02	25.55 ± 0.02 (3.04)	13.14 ± 0.02 (1.5)	28.10 ± 0.02 (3.3)	39.78 ± 0.02 (4.7)
Total precipitation over ocean (mm/year)	1,204.50 ± 0.02	31.00 ± 0.01 (2.5)	−7.25 ± 0.02 (−0.6)	29.14 ± 0.02 (2.4)	23.75 ± 0.02 (2.0)
Total precipitable water (kg m^{-2})	24.82 ± 0.03	3.80 ± 0.06 (15.3)	0.23 ± 0.05 (1.0)	4.14 ± 0.06 (16.7)	4.03 ± 0.09 (16.2)
Soil moisture (kg m^{-2})	103.9 ± 0.06	0.77 ± 0.08 (0.74)	1.86 ± 0.08 (1.8)	2.63 ± 0.08 (2.5)	2.63 ± 0.13 (2.5)
Run-off (mm/year)	258.76 ± 1.1	12.10 ± 1.71 (4.7)	24.57 ± 1.50 (9.5)	34.96 ± 1.90 (13.5)	36.70 ± 2.80 (14.2)
LAI	1.89 ± 0.01	−0.14 ± 0.01 (−7.2)	0.59 ± 0.01 (31.1)	0.46 ± 0.01 (24.2)	0.45 ± 0.01 (23.9)
Land surface albedo	0.270 ± 0.000	−0.006 ± 0.000 (−2.2)	−0.003 ± 0.000 (−1.1)	−0.008 ± 0.000 (−2.9)	−0.009 ± 0.000 (−3.3)
Fraction of ground covered by snow	0.23 ± 0.000	−0.013 ± 0.001 (−5.6)	−0.003 ± 0.001 (−1.3)	−0.02 ± 0.001 (−8.7)	−0.016 ± 0.001 (−6.9)
GPP (Gt-C/y)	136.3 ± 0.2	−3.59 ± 0.28 (−2.6)	34.04 ± 0.31 (25)	33.05 ± 0.27 (24.3)	30.45 ± 0.51 (22.3)
Autotrophic respiration (Gt-C/y)	89.4 ± 0.2	−0.54 ± 0.22 (−0.6)	22.82 ± 0.25 (25.5)	24.4 ± 0.21 (27.3)	22.28 ± 0.41 (24.9)
NPP (Gt-C/y)	46.9 ± 0.1	−3.05 ± 0.14 (−6.5)	11.22 ± 0.16 (23.9)	8.64 ± 0.16 (18.4)	8.17 ± 0.26 (17.4)
Heterotrophic respiration (Gt-C/y)	44.6 ± 0.02	−2.80 ± 0.05 (−6.3)	10.38 ± 0.07 (23.3)	7.94 ± 0.05 (17.8)	7.58 ± 0.08 (17)
Fire loss(Gt-C/y)	2.4 ± 0.03	−0.12 ± 0.04 (−4.8)	0.54 ± 0.05 (22.7)	0.64 ± 0.05 (26.8)	0.42 ± 0.08 (17.6)
NEE (Gt-C/y)	0.10 ± 0.12	0.14 ± 0.18	−0.29 ± 0.19	−0.05 ± 0.20	−0.15 ± 0.32
Soil respiration (Gt-C/y)	84.0 ± 0.1	−3 ± 0.10 (−3.6)	19.46 ± 0.15 (23.2)	17.63 ± 0.12 (21)	16.46 ± 0.20 (19.6)
Evapotranspiration (mm/year)	614.1 ± 0.8	7.99 ± 0.95 (1.3)	−19.31 ± 0.94 (−3.1)	−5.54 ± 0.90 (−0.9)	−11.32 ± 1.74 (−1.8)
Vegetation C (Gt-C)	717.5 ± 0.23	−59.2 ± 0.43 (−8.2)	258.4 ± 0.62 (36)	198.5 ± 0.29 (27.7)	199.2 ± 0.59 (27.8)
SOILC (Gt-C)	515.7 ± 0.11	−59.6 ± 0.16 (−11.5)	84.5 ± 0.31 (16.4)	28.1 ± 0.07 (5.5)	25.0 ± 0.16 (4.8)
Total ecosystem C (Gt-C)	1,322.6 ± 0.29	−131.2 ± 0.55 (−9.9)	370.5 ± 0.97 (28.0)	241.8 ± 0.3 (18.2)	239.3 ± 0.64 (18.1)

Uncertainty is given by the standard error computed from 100 annual means

* Direct effect = CO_2-fertilization plus CO_2-physiological effects

[†] Sum of CO_2-radiative and CO_2-direct effects (third and fourth columns)

[a] Values within parenthesis show the percentage changes relative to control

(2 × CO2). Soil organic matter and litter is decomposed by heterotrophic organisms and returned to the atmosphere by a process known as heterotrophic respiration (HR). A decline of 2.8 ± 0.05 Gt-C/year (6.3 %) in HR due to radiative effect is simulated in RAD. Previous transient climate change simulations have modeled an increase in HR due to climate-carbon cycle feedback (Bala et al. 2005; Boone et al. 1998; Cox et al. 2000; Cramer et al. 2001; Friedlingstein et al. 2001; Joos et al. 1991; Thompson et al. 2004). The response of HR to

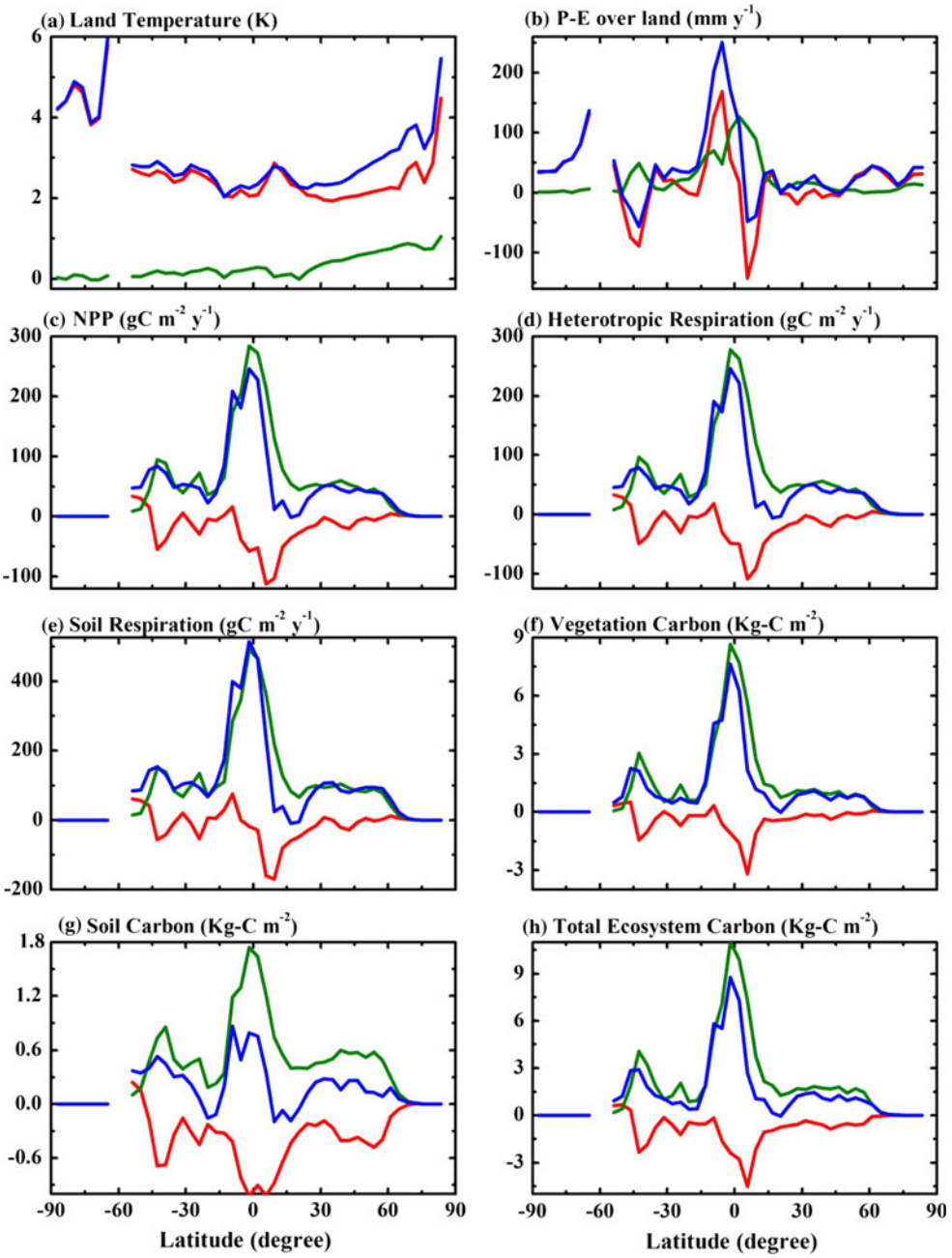

Fig. 2 Zonal mean changes of **a** surface air temperature over land, **b** precipitation minus evapotranspiration over land, **c** net primary productivity, **d** heterotrophic respiration, **e** soil respiration, **f** vegetation carbon, **g** soil carbon, **h** total ecosystem carbon for CO_2 radiative effect (*red line*), CO_2-direct effect (*green line*) and combined effect (*blue line*) with respect to control

climate warming would be to increase per unit soil carbon (i.e. the soil carbon residence time decreases), but by nature of our near-equilibrium simulation HR is constrained to equal NPP. Hence the net impact is to reduce soil carbon (Fig. 1u) with an associated decline in HR (Fig. 1k). For the CO_2-direct and combined effect, an increase of HR by 10.38 ± 0.07 Gt-C/year (23.3 %) and 7.94 ± 0.05 Gt-C/year (17.8 %), respectively, is simulated. The soil carbon residence time scale decreases from 11.6 years in 1 × CO_2 to 10.9 years for both CO_2-radiative (RAD) and CO_2–direct effects (BGC) in our equilibrium simulations.

Soil respiration (SR) is the sum of heterotrophic and root respiration. Therefore, its changes are similar to HR (Fig. 1m): SR declines by 3 ± 0.10 Gt-C/year (3.6 %) in association with radiative effect and increases by 19.46 ± 0.15 Gt-C/year (23.2 %) and 17.63 ± 0.12 Gt-C/year (21 %) for CO_2-direct effect and combined effects, respectively. The changes in SR are also similar to NPP. These results demonstrate the dominant role of pool size (which is of course determined by residence time scale) in determining changes in HR and SR under equilibrium climate change. NEE (net ecosystem exchange) is calculated by subtracting NPP from the sum of HR and Fire loss carbon:

$$\text{NEE} = \text{HR} + \text{Fire loss carbon} - \text{NPP} \quad (2)$$

Mean NEE is close to zero for equilibrium conditions (Fig. 1l). This relationship shows that HR should be the opposite of NPP for equilibrium conditions when NEE is nearly zero and fire losses are small.

The vegetation carbon is the total amount of carbon present in leaves, live stems, dead stems, fine roots, live and dead course roots of plants. It reduces roughly by 59.17 ± 1.51 Gt-C (8.3 %) in response to radiative effect and increases by 258.41 ± 2.66 Gt-C (36 %) in BGC because of CO_2-fertilization. For the combined effect, vegetation carbon increases by 198.5 ± 0.50 Gt-C (27.7 %). Soil carbon decreases 59.55 ± 1.39 Gt-C (11.5 %) due to radiative effect, and increases by 84.52 ± 5.01 Gt-C (16.4 %) and 28.13 ± 0.24 Gt-C (5.4 %), respectively, for CO_2-direct effect and combined effect respectively. In our experiments, since N-deposition rate is fixed, we find that the main drivers influencing the changes in total ecosystem N are biological nitrogen fixation and denitrification (Fig. S2). Increased vegetation N (Fig. 1t) and soil N (Fig. 1v) and hence total ecosystem N (Fig. 1x) are simulated in the BGC case while there are reductions in these variables in the RAD case.

Total ecosystem carbon (TEC) is the sum of all terrestrial carbon pools, such as vegetation carbon, soil carbon and litter carbon. TEC decreases by 131.21 ± 3.56 Gt-C (9.9 %) due to CO_2-radiative effect and increases by 370.46 ± 9.92 Gt-C (28 %) because of CO_2 fertilization. These changes in TEC have consequences for land-uptake related implied emissions in the CO_2-radiative and CO_2-direct effect cases for stabilizing atmospheric CO_2 at twice the pre-industrial levels in the absence of ocean uptake. For combined radiative and CO_2 fertilization effects the total ecosystem carbon increases by 241.75 ± 0.76 Gt-C (18.3 %). In SRES A2 scenario the atmospheric CO_2 concentration of 570 ppm is reached around year 2070 and total amount of carbon emitted by that time will reach 1250 Gt-C (Bala et al. 2005; Gillett et al. 2011) suggesting that the upper bound for cumulative carbon emission sequestration in the terrestrial ecosystems by 2070 (when atmospheric CO_2 doubled relative to preindustrial times) is only about 20 % of the cumulative emissions.

There is a decline of more than 4 kg-C m^{-2} in TEC (Fig. 3) in the Amazon, tropical African and Southeast Asian forest in RAD and a decrease of up to 2 kg-C m^{-2} in the temperate forests of Eurasia and North America. In the response to CO_2-physiological and -fertilization effect (BGC), Amazon, Southeast Asian, and tropical African forests gain TEC larger than 10 kg-C m^{-2} and increase up to 8 kg-C m^{-2} in temperate forests of Eurasia and North America. In the combined case (2 × CO_2), TEC increases are similar to BGC. Figure 2f–h show that the vegetation C

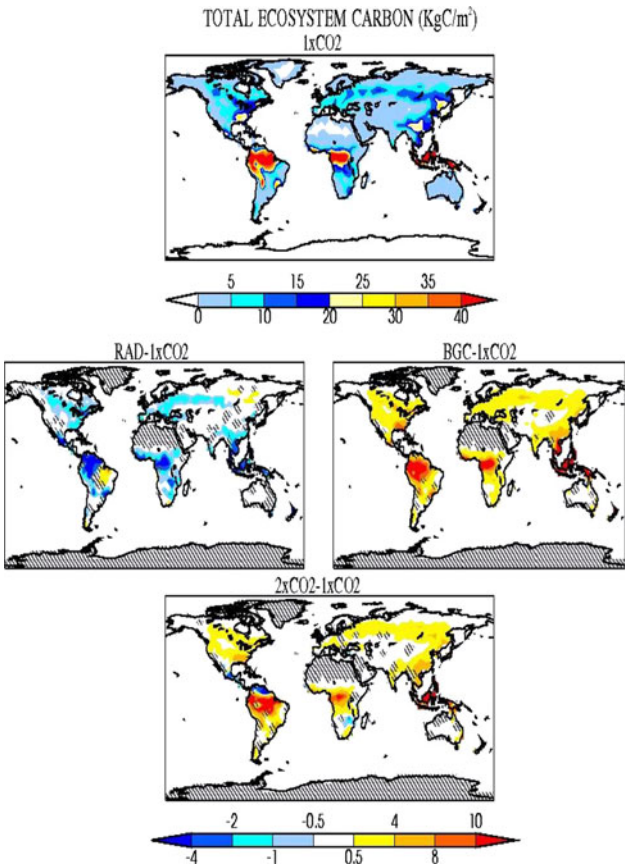

Fig. 3 Total ecosystem carbon (TEC) in the control simulation (*top panel*), and changes in TEC for radiative effect (middle panel, *left*), CO_2-direct effect (middle panel, *right*) and for the combined effect (*bottom panel*). The *hatching* indicates regions where the changes are not significant at the 99 % level of confidence. Significance level is estimated using a Student *t* test with sample of 100 annual means and standard error corrected for serial correlation (Zwiers and von Storch 1995)

is the main contributing factor for the changes in TEC rather than soil C. This may be a model artifact since soil carbon pool size is underestimated in this model (~550 Gt-C vs. the conventionally accepted value of 1,500 Gt-C) (Bonan and Levis 2010). This underestimate is associated with a faster turnover time scale in this model. If the soil carbon pool is trebled to match with accepted values, then soil carbon changes for both direct-CO_2 and radiative effects would be thrice the values simulated in this study.

4.2 Carbon storage sensitivity

In this section, we estimate the climate-carbon cycle and concentration-carbon feedback factors and the carbon storage sensitivity to elevated CO_2 and to temperature. The climate-carbon cycle feedback represents the CO_2-radiative effect on carbon uptake whereas the concentration-carbon

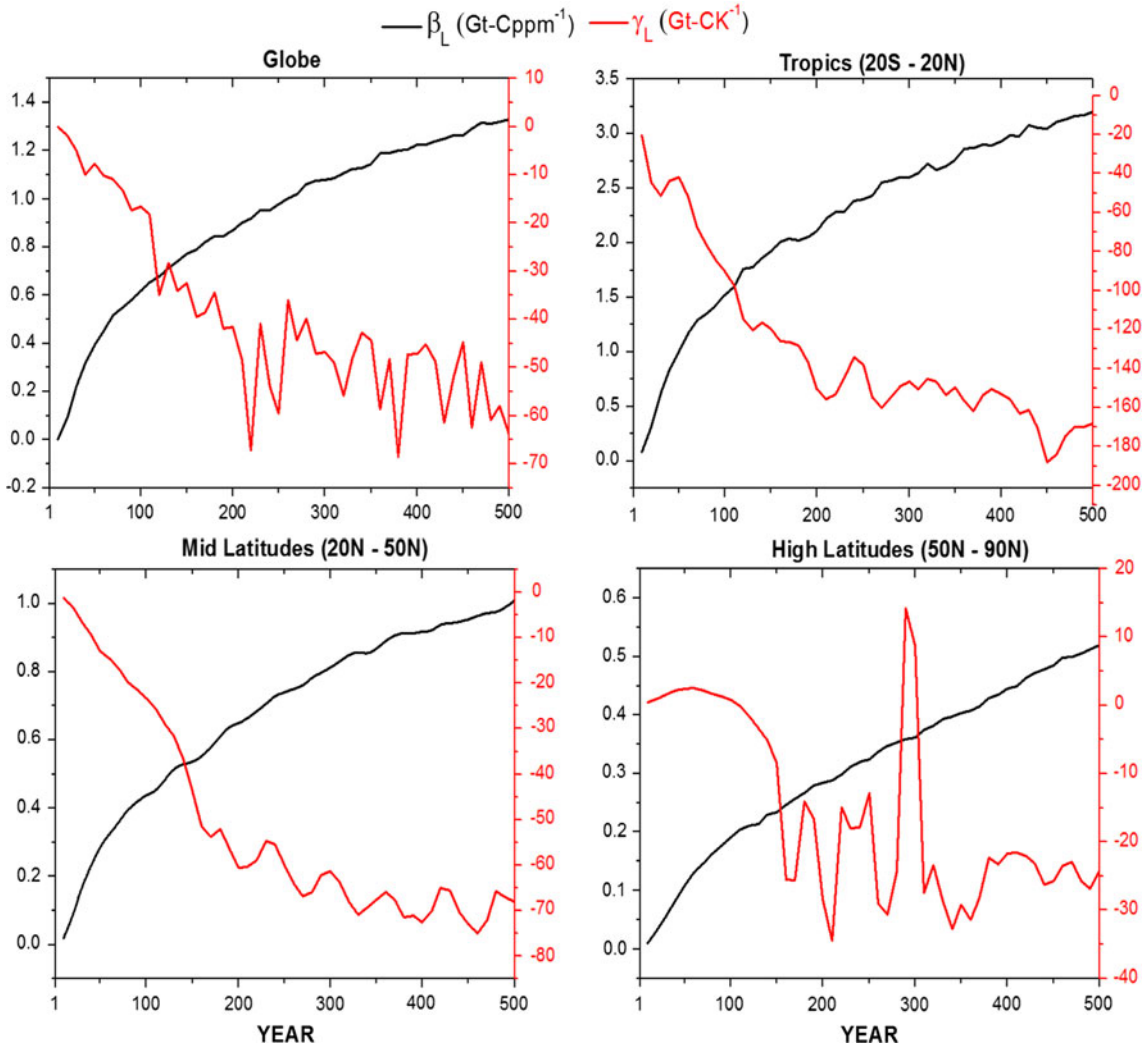

Fig. 4 Evolution of Terrestrial carbon storage sensitivity to atmospheric CO_2 (beta,β_L; *black line*) and to temperature (gamma, γ_L; *blue line*) for constant preindustrial N deposition for the global domain, tropics, mid- and high-latitudes

feedback represents the CO_2-direct effect on uptake. For our specified CO_2 simulations, following Plattner et al. (2008) and Zickfeld et al. (2011), we estimate the feedback factor as the ratio in implied cumulative emissions for simulations with a specific feedback on and off:

$$F = \frac{\Delta C_E^{on}}{\Delta C_E^{off}} \tag{3}$$

where ΔC_E is the cumulative carbon emission relative to the control run. For the climate-carbon cycle feedback, this feedback parameter is estimated as the ratio of the changes in TEC in the $2 \times CO_2$ case to BGC, and the ratio in the $2 \times CO_2$ case to RAD yields the concentration-carbon feedback. We estimate them as 0.65 and 1.84, indicating that climate-carbon feedback is positive (positive feedback is associated with lower implied emissions and $F < 1$) and concentration-carbon feedback is negative which in agreement with earlier studies (Friedlingstein et al. 2006; Govindasamy et al. 2005; Zickfeld et al. 2011): radiative effect enhances the atmospheric CO_2 increase and hence climate change whereas CO_2-fertilization dampens CO_2 increase and climate change.

The carbon storage sensitivity over land (β_L) to CO_2 is defined as the change in total ecosystem carbon (TEC) associated with unit change in atmospheric CO_2 (C_a). The carbon storage sensitivity over land to temperature (γ_L) is defined as the change in total ecosystem carbon associated with unit change in temperature due to radiative effect. The carbon storage sensitivities β_L and γ_L are diagnosed from the difference in TEC between simulations (Friedlingstein et al. 2006; Friedlingstein et al. 2003):

Table 2 Numerical values of β_L and γ_L simulated by previous studies

References	Model	Scenarios used	C/CN	β(Gt-C/ppm)	γ(Gt-C/K)
Friedlingstein et al. (2006)	HadCM3LC	SRES A2	C	1.3	−177
	IPSL-CM2C			1.6	−98
	IPSLCM4-LOOP			1.3	−20
	CSM-1			1.1	−23
	MPI			1.4	−65
	LLNL			2.8	−70
	FRCGC			1.2	−112
	UMD			0.2	−40
	Uvic-2.7			1.2	−98
	CLIMBER			1.1	−57
	BERN-CC			1.6	−105
	All Models Average			1.35	−79
Sitch et al. (2008)	HYL	SRES A2	C	1.48–1.94	−60 to −198
	LPJ	A1F1		1.36–1.75	−61 to −203
	ORCHIDEE	B1		2.13–3.36	−62 to −229
	Sheffield-DGVM	B2		1.87–2.70	−67 to −208
	TRIFFID				
Bonan and Levis (2010)	CLM4	Historical CO_2 from 1973 to 2004	C	0.92–0.94	−11 to −11.7
			CN	0.24–0.26	−0.2 to 0.3
Zaehle et al. (2010)	O-CN	SRES A2	C	1.27	−61
			CN	−0.63	−51
Thornton et al. (2007)	CLM3.0	Historical period from 1850–2000 followed by SRES A2	C	1.4–2.5	∼ −3.2 to −3.7
			CN	0.4–0.9	∼ −0.8
Thornton et al. (2009)	CCSM3	SRES A2	CN	0.5	−25
Zickfeld et al. (2011)	UVic ESCM	SRES A2	C	1.12–1.32	−87 to −137
Frank et al. (2010)	Observational	Last millennium	–	–	−3.6 to −45.0[a]
This study	CCSM4	2 × CO_2	CN	1.3	−53.77

[a] The observational value corresponds to γ of the global carbon cycle (γ of land plus γ of ocean)

$$\beta_L = \frac{\Delta TEC}{\Delta C_a} = \frac{TEC_{BGC} - TEC_{1\times CO_2}}{C_{a(BGC)} - C_{a(1\times CO_2)}} \quad (4)$$

$$\gamma_L = \frac{\Delta TEC}{\Delta T} = \frac{TEC_{RAD} - TEC_{1\times CO_2}}{T_{RAD} - T_{1\times CO_2}} \quad (5)$$

β_L and γ_L are measures of terrestrial carbon cycle sensitivity to CO_2 and climate changes, respectively (Boer and Arora 2009; Zickfeld et al. 2011). C_a and T refer to atmospheric CO_2 concentrations and global-mean surface temperature.

Figure 4 shows the evolution of β_L and γ_L over 500 years of simulation. We have used the cumulative increase in TEC since the start of the simulations for calculating both β_L and γ_L at any point in time. Our estimates are similar to previous studies which used single summary values based on differences between the values of carbon and temperature state variables at the beginning and end of simulations (Friedlingstein et al. 2006) except that we compute the temporal evolution of the parameters by estimating the cumulative changes at annual intervals. Thornton et al. (2009) use linear regression between cumulative carbon stock changes and state variables (CO_2 and temperature) at annual intervals to evaluate temporal evolution of β_L and γ_L.

β_L for the global domain is positive since CO_2-fertilization leads to an increase in TEC in the absence of climate warming and γ_L is negative since climate warming results in reduced NPP and the consequent declines in vegetation and soil carbon. We note an increase in the magnitude of both β_L and γ_L with time. While γ_L reaches a steady mean value after about 200 years in response to climate warming, β_L has not reached steady value even after 500 years likely because of the interactive N-cycle and the consequent nitrogen limitation. The drift in TEC (Fig. 1w), total ecosystem nitrogen (Fig. 1x) and the drift in β_L (Fig. 4a) nearly match. The mean values in the last 100 years for β_L is 1.301 Gt-C ppm^{-1} and −53.77 Gt-C K^{-1} for γ_L. These equilibrium values should be compared

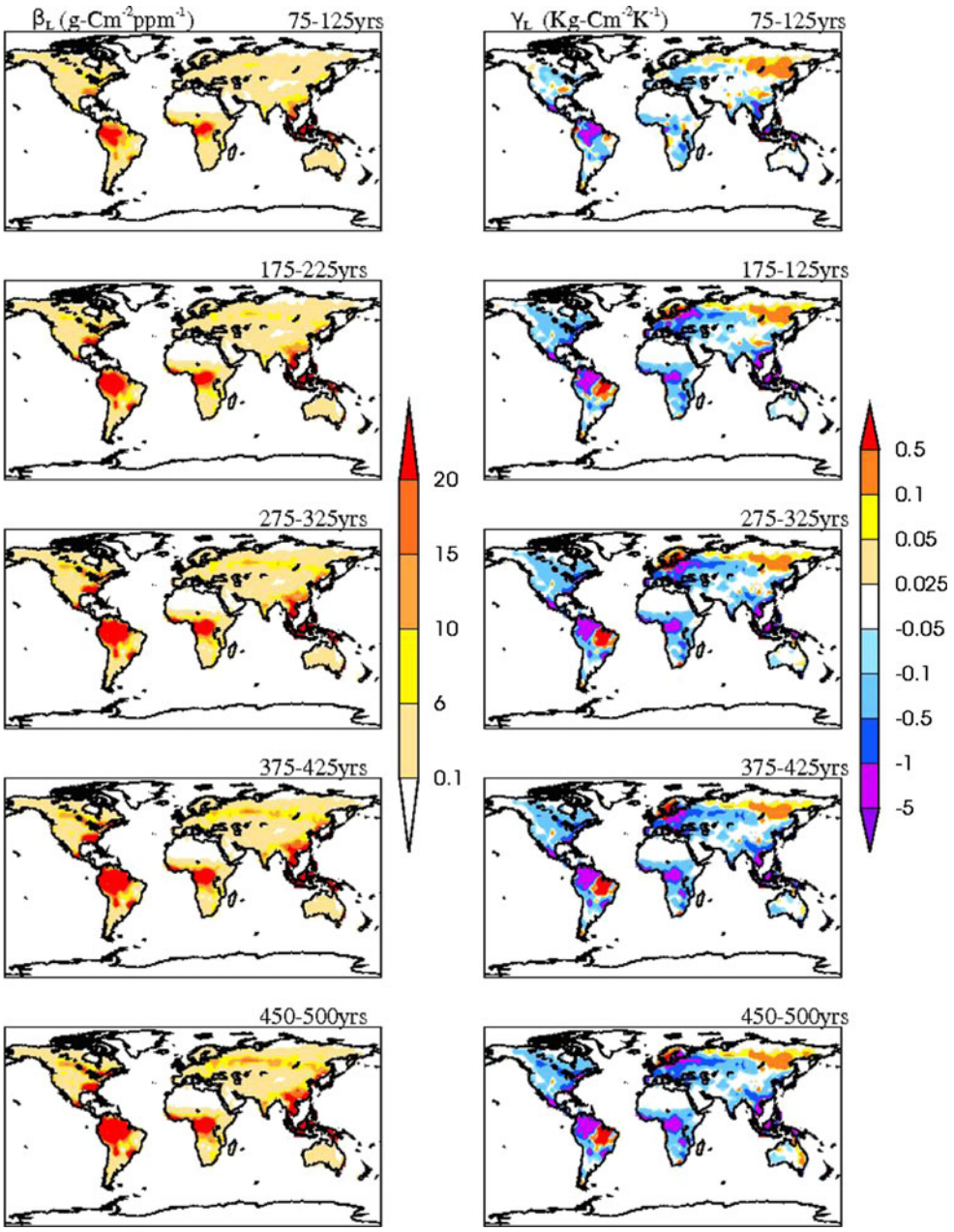

Fig. 5 Spatial pattern of the evolution of the sensitivity of terrestrial carbon storage to atmospheric CO_2 (beta, β_L; *left panels*) and temperature (gamma, γ_L; *right panels*)

to 0.2–0.5 Gt-C ppm^{-1} for β_L and -12 to -25 Gt-C K^{-1} for γ_L reported in earlier studies using the same model but in transient simulations (Bonan and Levis 2010; Thornton et al. 2009). The increasing magnitudes of β_L and γ_L with time (Fig. 4) suggest that previous transient simulations using CCSM for various scenarios obtained lower values of β_L and γ_L because they were not equilibrium simulations. Larger values of β_L and γ_L in the tropical region primarily control the β_L and γ_L for the global domain (Fig. 4). The dependence of β_L on emission scenario and hence on state variables other than CO_2 concentration has been previously noted (Boer and Arora 2009).

The values of β_L and γ_L estimated in previous model studies including carbon-only or carbon–nitrogen dynamics in the land model are listed in Table 2. There are large variations in β_L and γ_L values among the models. When compared with previous CCSM simulations (Thornton et al. 2009) and stand-alone-land model (CLM) simulations (Bonan and Levis 2010; Thornton et al. 2007), our equilibrium sensitivity values are larger. In our BGC simulation, TEC increases by 370 Gt-C after 400 years of stabilization for $\sim$285 ppm increase in atmospheric CO_2. However, prior studies using CLM which have used transient increase in atmospheric CO_2 do not show such large

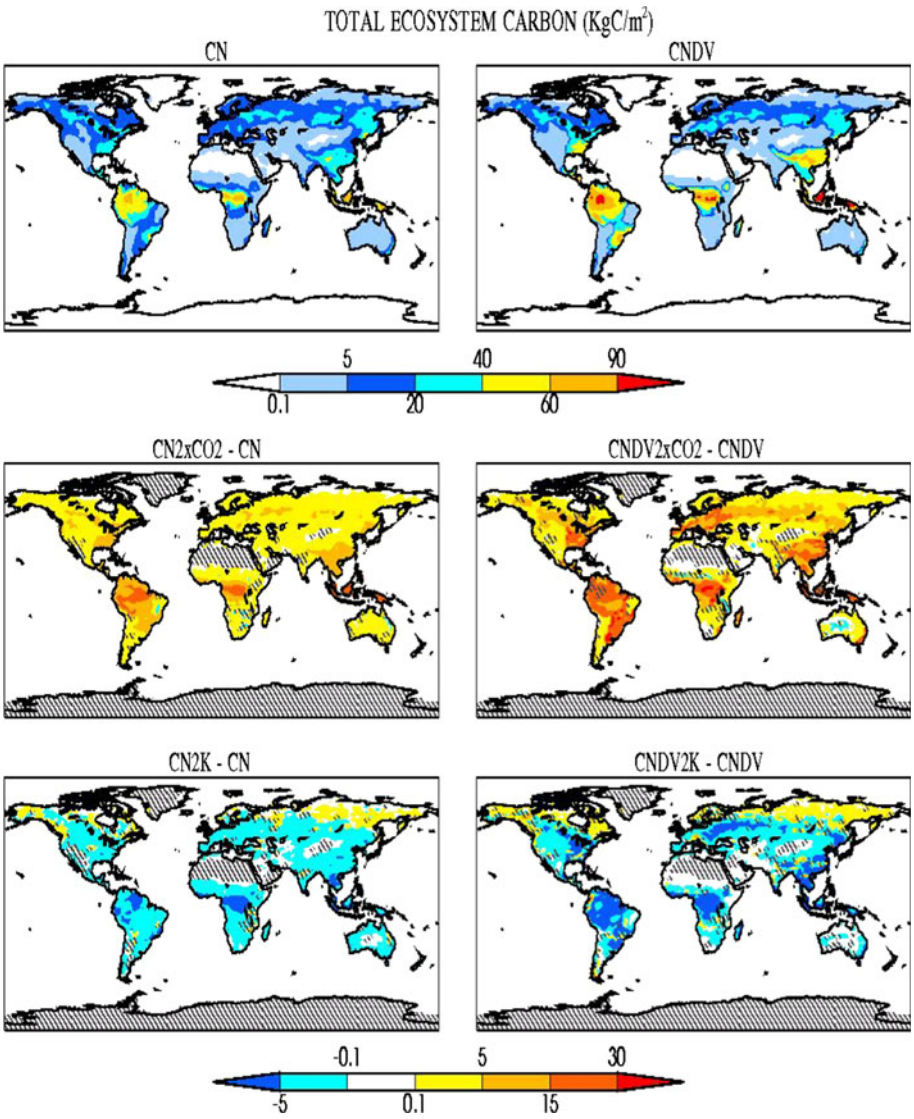

Fig. 6 Total ecosystem carbon (TEC) in the control CN and CNDV simulations (*top panels*), and changes in TEC for CO_2-direct effect (*middle panels*) and radiative effect (*bottom panels*) in the last 100 years of 600 year offline CN (*left panels*) and CNDV (*right panels*) simulations. The *hatching* indicates regions where the changes are not significant at the 99 % level of confidence. Significance level is estimated using a Student *t* test with sample of 100 annual means and standard error corrected for serial correlation (Zwiers and von Storch 1995)

increases in TEC: total carbon stock change of only about 281 Gt-C for the stand-alone CLM3.0-CN is simulated for a transient CO_2 change from 283.6 to 843.6 ppm under constant nitrogen deposition and constant climate (Thornton et al. 2007); offline simulations using CLM4 (Bonan and Levis 2010) show about 10 Gt-C stock increase for a 42 ppm transient CO_2 increase with constant nitrogen deposition with a β_L value of 0.25 Gt-C per ppm; fully coupled transient CCSM4 simulations (Thornton et al. 2009) show an increase of less than 250 Gt-C for CO_2 increase from 287 to 884 ppm under constant nitrogen deposition and constant climate. Therefore our study demonstrates that β_L is a time dependent quantity and its equilibrium values are much larger than transient values because of lags in the climate system. γ_L also has time dependence (Fig. 4). The near-stabilization of γ_L after about 200 years (Fig. 4) is an indication that the time scale of terrestrial carbon cycle response to CO_2-radiative effect is about 200 years in our model. However, the evolution of β_L indicates that the response time scale for CO_2-direct effect is more than 500 years.

Figure 5 shows the time evolution of the spatial pattern of β_L and γ_L. The magnitudes are higher in the thickly vegetated regions: Amazon, central Africa, Europe, northeastern North America, Southeast Asia and Boreal forests. While β_L is uniformly positive everywhere, γ_L is both positive and negative. Warming leads to reduced TEC in most regions (negative γ_L) except in the boreal forest regions where warming leads to longer growing season and hence more TEC. Though γ_L is negative (<-5 kg-C m^{-2} K^{-1}) over Amazon, it is positive (>0.5 kg-C m^{-2} K^{-1}) in the southeastern region adjacent to Amazon where we find that there is tropical deciduous forest and rainfall increases there in our model under climate change. The sensitivity to temperature increases from low values to about 100 g-C m^{-2} K^{-1} in the northern part of Eurasia by

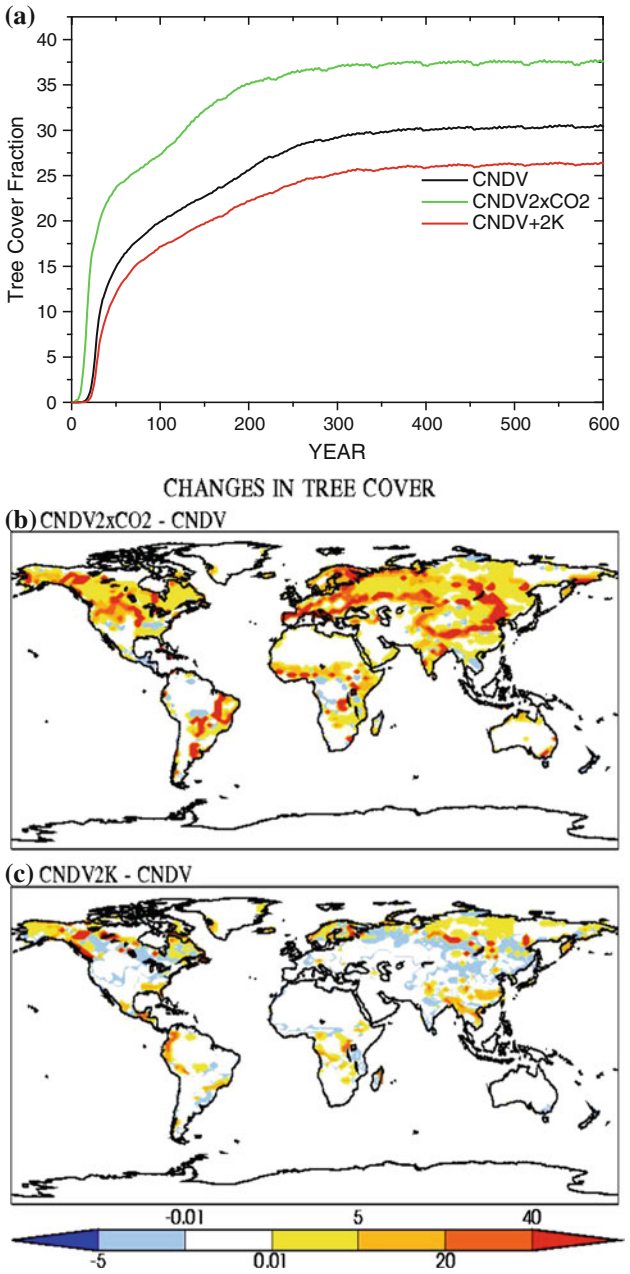

Fig. 7 **a** Evolution of the global mean tree cover fraction in the dynamic vegetation simulations and the mean spatial pattern of changes in tree cover fraction in the last 100 years for **b** CO_2-direct effect (CNDV2 × CO2-CNDV) and **c** climate effect (CNDV2K-CNDV)

the end of simulation. Evolution of β_L shows an expansion of regions with higher values with time (most notable in the Amazon).

4.3 Sensitivity to dynamic vegetation changes

Since our main aim is to estimate the maximum land uptake of carbon over longer time scales, it is important to evaluate the sensitivity of our estimate to dynamic changes in vegetation which operates on a time scale of multiple centuries. In this section, we briefly discuss the sensitivity of our results to vegetation dynamics. Since the dynamic vegetation component of CLM4 has not been evaluated in a fully coupled framework, we use the offline version of CLM4 to study the sensitivity of terrestrial carbon uptake for dynamic changes in vegetation. We perform six 600-year experiments: (1) "CN", a control offline simulation with prescribed 1,850 levels of CO_2 and N-deposition, (2) "CN2 × CO_2", same as CN but with doubled CO_2. (3) "CN2K", same as CN simulation but with a uniform increase of 2K for the atmospheric temperature forcing to mimic approximately the climate change simulated in our CCSM4 RAD experiment, (4) CNDV, (5) CNDV2 × CO2 and (6) CNDV2K are similar to (1), (2) and (3), respectively, but with dynamic vegetation. It should be noted that we have imposed only temperature changes in (3) and (6) but corresponding changes in other variables such as precipitation, clouds, humidity are not imposed. We recognize the importance of changes in these variables for carbon cycle changes and plan to address this issue in a future study.

All the six experiments are driven by a 57 year (1948–2004) observation-constrained atmospheric forcing dataset (Qian et al. 2006). When forced by this dataset, CLM4CN reproduces many aspects of the long term mean annual cycle, inter-annual and decadal variations, and trends of stream flow for many large rivers (Oleson et al. 2008). Since the simulations reach near-equilibrium state after 500 years (NEE is nearly zero), we use the averages in the last 100 years for investigating the sensitivity to dynamic vegetation (Fig. 6).

We find an increase in fractional cover of global (tropical, temperate and boreal) forests due to CO_2 fertilization (Fig. 7a) which is in good agreement with an earlier study (Bala et al. 2006), whereas there is a decline of tree cover due to climate warming (Fig. 7b). The total forested fractional area increases by 8.2 % and decreases by 4.4 % (Fig. 7c), respectively, for CO_2-direct effect (CNDV2 × CO_2-CNDV) and warming effect (CNDV2K-CNDV). Large changes in tree cover are simulated in North America and Eurasia for both effects. There is an expansion of Boreal forests (about 3 %) for CO_2 direct effect (Fig. 7b) and for the climate effect there is a decline of about 1.4 %. Changes in forest fraction are also visible in the periphery of existing forests in the Amazon and Central Africa (Fig. 7).

The global value of TEC changes for the last 100 years of simulations are shown in Table 3 and spatial patterns are shown in Fig. 6. We find that TEC in CNDV control is higher than in CN control by 382 Gt-C which is in good agreement with a recent CLM4 study (Castillo et al. 2011) that also simulated a larger TEC in CNDV than in CN

Table 3 Global and annual mean changes in carbon stocks in Gt-C for the last 100 years of 600 year CCSM4 and offline CN and CNDV simulations

		CCSM4	CN	CNDV	CNDV-CN
Total ecosystem C (Gt-C)	Control	1,322.6	1,824.6	2,206.8	382.2 (20.9)
	CO_2 fertilization effect	370.5 (28.0[a])	487.9 (26.7)	918.2 (41.6)	430.3 (88.2)
	Climate effect	−131.2 (−9.9)	−260.6 (−14.3)	−446.9 (−20.2)	−186.3 (−71.5)
Total vegetation C (Gt-C)	Control	717.5	1,002.0	1,570.2	568.2 (56.7)
	CO_2 fertilization effect	258.4 (36.0)	351.9 (35.0)	738.6 (47.0)	386.7 (109.9)
	Climate effect	−59.6 (−8.2)	−180.1 (−18)	−371.8 (− 23.0)	−191.7 (−106.5)
Soil C (Gt-C)	Control	515.7	695.7	522.9	−172.8 (−24.8)
	CO_2 fertilization effect	84.5 (16.0)	102.5 (14.7)	126.6 (24.0)	24.1 (23.5)
	Climate effect	−59.6 (−11.0)	−64.1 (−9)	−53.6 (−10.0)	10.5 (16.4)
β_L		1.3	1.7	3.3	1.54 (88.5)
γ_L		−53.8	−130.3	−223.5	−93.2 (−71.5)

[a] Values within parenthesis show the percentage changes relative to control

(1,878 vs. 1,526 Gt-C). We find that the spatial pattern of TEC in CNDV is similar to CN but the magnitudes are larger (Fig. 6). Simulated vegetation carbon (soil carbon) is much larger (smaller) in CNDV than in CN. The changes in TEC for CO_2-direct and radiative effects are amplified by 88 and 72 %, respectively, in CNDV when compared to CN suggesting that β_L and γ_L are larger in CNDV than in CN by similar percentages (Table 1). We do not find major shifts in vegetation types for both CO_2-direct and -radiative effects: hotspots of change (i.e. Amazon, Central Africa, and Eastern Asia) remain the same in CNDV and CN. A detailed investigation of the causes for the larger response in CNDV is beyond the scope of this paper and will be the subject of a future paper.

5 Conclusions

We have investigated the sensitivity of total ecosystem carbon to the effects of radiative effect, CO_2-physiological and CO_2-fertilization effects, and the combined effects, for a doubling of CO_2 concentration. The CO_2-physiological effect refers to the reduced opening of stomata in leaves for elevated CO_2-levels. The CO_2-fertilization effect refers to the stimulated photosynthesis and the associated increases in leaf area index (LAI), net primary productivity (NPP), and carbon stocks in leaves, stems and roots. We obtain an increase of 2.14 K in global and annual mean temperature as response to radiative effect and 0.22 K increase as the response to the CO_2-direct effect (i.e., the combined CO_2-physiological and CO_2-fertilization effects). The CO_2-physiological effect induces a reduction in transpiration and as a consequence low clouds, leading to land surface warming (Betts et al. 2007; Cao et al. 2010) whereas the CO_2-fertilization effect induces increases in LAI which would tend to offset some of this warming by increasing canopy transpiration. LAI increase could also lower the surface albedo and enhance the warming caused by physiological effect. Net primary productivity (NPP) increases by about 24 % due to the CO_2-direct effect on the land biosphere and decreases by about 7 % due to CO_2-radiative effect on climate. The terrestrial ecosystem carbon (TEC), which is the sum of soil, vegetation, and litter pools, increases by 28 % from the CO_2-direct effect, decreases by 10 % from the radiative effect and increases by 18 % from the combined effects. Our results show that the responses to CO_2-radiative and CO_2-direct effects are roughly additive: the combined effect can be well-represented by linear sum of these two effects (Table 1).

Using an offline version of land model, we have also investigated the sensitivity of total ecosystem carbon to CO_2-direct and -radiative effects when dynamics changes in vegetation are allowed. We find that the changes in total ecosystem carbon for CO_2-direct and radiative effects are amplified by 88 and 72 % (Table 3), respectively, in dynamic vegetation simulations when compared to simulations without dynamic vegetation. We find large changes in fractional tree cover in the dynamic vegetation simulations which are likely the primarily cause for larger sensitivities.

Previous studies using CLM have shown that terrestrial carbon sequestration was overestimated when carbon and nitrogen cycle (CN) interactions were not considered (Bonan and Levis 2010; Thornton et al. 2007). Though our study using CLM has CN interactions, our results are limited by the prescription of constant pre-industrial nitrogen deposition. However, the results obtained for carbon storage sensitivities are well within the range of

other models which do not include CN interactions (Table 2), suggesting the huge uncertainties in model-based estimates of concentration-carbon cycle and climate-carbon cycle feedback parameters. Further, it has been shown in some observations that increased nitrogen deposition is unlikely to influence the CO_2 sinks in forests (Nadelhoffer et al. 1999).

One of the main limitations of this work is that CLM4 (like many other global land models) does not have representation of high latitude permafrost carbon reservoir which contains large quantity of organic carbon matter because of low temperatures in the high latitudes. As global temperature increases due to climate change, the thawing of permafrost could result in microbial decomposition of frozen organic carbon and eventually this region could become a large source of CO_2 (Schuur et al. 2008; Schuur et al. 2009). This positive feedback of soil carbon respiration to global warming scenario is not simulated by CLM4. If this effect is included in the land model, the magnitude of γ_L is likely to increase. Another limitation is that the oceanic component of the carbon cycle is not represented in our study. However, because we are framing our study in terms of analyzing the response to a specified change in atmospheric CO_2 concentration, the inclusion of ocean carbon cycle in simulations with prognostic atmospheric CO_2 would not change the values of β_L and γ_L and hence would not alter the main conclusions of this study. Our primary conclusion is that the land carbon cycle sensitivities to both changes in CO_2 concentration and temperature previously estimated from short transient simulations are smaller than equilibrium values due to long time constants associated with carbon accumulation in the terrestrial biosphere.

Previous modeling studies, using transient simulations, have found differing values of carbon storage sensitivity for temperature (γ_L) and elevated CO_2 (β_L) (Table 2) which suggests the large uncertainty in model-based estimates of the climate- and concentration-carbon cycle feedbacks. In addition, we find that the equilibrium values of these parameters have larger magnitudes when compared to estimates based on transient simulations using the same model (Bonan and Levis 2010; Thornton et al. 2009). Many models have transient β_L and γ_L values which are about the same or larger than equilibrium sensitivities as simulated by our model (Table 2). The implication from our study is that the equilibrium sensitivities of the models shown in Table 2 are likely to be much larger than the values we have found for CLM4. This suggests a large spread in equilibrium terrestrial carbon cycle sensitivity to CO_2 emissions. Improved knowledge on the potential sequestration of carbon in terrestrial ecosystem would require narrowing down the uncertainty in our estimate of the concentration- and climate-carbon cycle feedback parameters.

Acknowledgments We thank Drs. Chris Jones and Sam Levis for their critical comments and suggestions which helped us to improve the original manuscript substantially. Financial support from Department of Science and Technology under the grant DST 0948 is gratefully acknowledged. Dr. Devaraju and Mr. Krishna are supported by the Divecha Center for Climate Change.

References

Bala G, Caldeira K, Mirin A, Wickett M, Delire C (2005) Multiceutury changes to the global climate and carbon cycle: results from a coupled climate and carbon cycle model. J Clim 18(21):4531–4544

Bala G et al (2006) Biogeophysical effects of CO_2 fertilization on global climate. Tellus Ser B Chem Phys Meteorol 58(5):620–627

Betts RA et al (1997) Contrasting physiological and structural vegetation feedbacks in climate change simulations. Nature 387(19):796–799

Betts RA et al (2004) The role of ecosystem-atmosphere interactions in simulated Amazonian precipitation decrease and forest dieback under global climate warming. Theor Appl Climatol 78(1–3):157–175

Betts RA et al (2007) Projected increase in continental runoff due to plant responses to increasing carbon dioxide. Nature 448(7157): 1037–1041

Boer GJ, Arora V (2009) Temperature and concentration feedbacks in the carbon cycle. Geophys Res Lett 36:L02704. doi:10.1029/2008GL036220

Bonan GB, Levis S (2010) Quantifying carbon-nitrogen feedbacks in the Community Land Model (CLM4). Geophys Res Lett 37:L0740. doi:10.1029/2010GL042430

Boone RD, Nadelhoffer KJ, Canary JD, Kaye JP (1998) Roots exert a strong influence on the temperature sensitivity of soil respiration. Nature 396(6711):570–572

Cao L, Bala G, Caldeira K, Nemani R, Ban-Weiss G (2010) Importance of carbon dioxide physiological forcing to future climate change. Proc Natl Acad Sci USA 107(21):9513–9518

Castillo CKG, Levis S, Thornton P (2011) Evaluation of the new cndv option of the community land model: effects of dynamic vegetation and interactive nitrogen on CLM4 means and variability. J Clim 25:3702–3714

Collatz GJ, Ribas-Carbo M, Berry JA (1992) Coupled photosynthesis-stomatal conductance model for leaves of C4 plants. Aust J Plant Physiol 19(5):519–538

Cox PM et al (1999) The impact of new land surface physics on the GCM simulation of climate and climate sensitivity. Clim Dyn 15(3):183–203

Cox PM, Betts RA, Jones CD, Spall SA, Totterdell IJ (2000) Acceleration of global warming due to carbon-cycle feedbacks in a coupled climate model. Nature 408(6809):184–187

Cramer W et al (2001) Global response of terrestrial ecosystem structure and function to CO_2 and climate change: results from six dynamic global vegetation models. Glob Change Biol 7(4): 357–373

Curtis PS (1996) A meta-analysis of leaf gas exchange and nitrogen in trees grown under elevated carbon dioxide. Plant, Cell Environ 19(2):127–137

Frank CD, Esper J, Raible CC, Buntgen U, Trouet V, Stosker B, Joos F (2010) Ensemble reconstruction constraints on the global carbon cycle sensitivity to climate. Nature 463:527–530

Friedlingstein P et al (2001) Positive feedback between future climate change and the carbon cycle. Geophys Res Lett 28(8): 1543–1546

Friedlingstein P, Dufresne JL, Cox PM, Rayner P (2003) How positive is the feedback between climate change and the carbon cycle? Tellus Ser B Chem Phys Meteorol 55(2):692–700

Friedlingstein P et al (2006) Climate-carbon cycle feedback analysis: results from the (CMIP)-M-4 model intercomparison. J Clim 19(14):3337–3353

Gedalof Z, Berg AA (2010) Tree ring evidence for limited direct CO(2) fertilization of forests over the 20th century. Glob Biogeochem Cycles 24:GB3027. doi:10.1029/2009GB003699

Gedney N et al (2006) Detection of a direct carbon dioxide effect in continental river runoff records. Nature 439(7078):835–838

Gent PR et al (2011) The Community Climate System Model Version 4. J Clim 24(19):4973–4991

Gillett NP, Arora VK, Zickfeld K, Marshall SJ, Merryfield AJ (2011) Ongoing climate change following a complete cessation of carbon dioxide emissions. Nat Geosci 4(2):83–87

Good P, Jones C, Jason L, Betts R, Booth B, Huntingford C (2011) Quantifying environmental drivers of future tropical forest extent. J Clim 24:1337–1349

Govindasamy B et al (2005) Increase of carbon cycle feedback with climate sensitivity: results from a coupled climate and carbon cycle model. Tellus Ser B Chem Phys Meteorol 57(2):153–163

House JI, Prentice IC, Ramankutty N, Houghton RA, Heimann M (2003) Reconciling apparent inconsistencies in estimates of terrestrial CO_2 sources and sinks. Tellus Ser B Chem Phys Meteorol 55(2):345–363

Jones C, Jason L, Spencer L, Betts R (2009) Committed terrestrial ecosystem changes due to climate change. Nat Geosci 2:484–487

Jones C, Jason L, Spencer L, Betts R (2010) Role of terrestrial ecosystems in determining CO_2 stbilization and recovery behaviour. Tellus Ser B Chem Phys Meteorol 62(5):682–699

Joos F, Sarmiento JL, Siegenthaler U (1991) Estimates of the effect of Southern-Ocean iron fertilization on atmospheric CO_2 concentrations. Nature 349(6312):772–775

Kloster S et al (2010) Fire dynamics during the 20th century simulated by the Community Land Model. Biogeosciences 7(6):1877–1902

Lawrence DM et al (2011) Parameterization improvements and functional and structural advances in version 4 of the Community Land Model. J Adv Model Earth Syst 3:1–29. doi:10.1029/2011MS000045

Le Quere C et al (2009) Trends in the sources and sinks of carbon dioxide. Nat Geosci 2(12):831–836

Levis S, Bonan GB, Vertenstein M, Oleson KW (2004) The Community Land Model's dynamic global vegetation model (CLM-DGVM): technical description and user's guide. NCAR, Boulder

Lloyd J, Taylor JA (1994) On the temperature-dependence of soil respiration. Funct Ecol 8(3):315–323

Matthews HD (2007) Implications of CO(2) fertilization for future climate change in a coupled climate-carbon model. Glob Change Biol 13(5):1068–1078

Matthews HD, Weaver AJ, Meissner KJ (2005) Terrestrial carbon cycle dynamics under recent and future climate change. J Clim 18(10):1609–1628

Nadelhoffer KJ et al (1999) Nitrogen deposition makes a minor contribution to carbon sequestration in temperate forests. Nature 398(6723):145–148

Norby RJ et al (2005) Forest response to elevated CO_2 is conserved across a broad range of productivity. Proc Nat Acad Sci USA 102(50):18052–18056

Oleson KW et al (2008) Improvements to the Community Land Model and their impact on the hydrological cycle. J Geophys Res 113:G01021. doi:10.1029/2007JG000563

Oleson KW, Bonan GB, Feddema JJ, Vertenstein M, Kluzek E (2010) Technical description of an urban parameterization for the Community Land Model (CLM). NCAR, Boulder

Owensby CE, Ham JM, Knapp AK, Auen LM (1999) Biomass production and species composition change in a tallgrass prairie ecosystem after long-term exposure to elevated atmospheric CO_2. Glob Change Biol 5(5):497–506

Plattner GK et al (2008) Long-term climate commitments projected with climate-carbon cycle models. J Clim 21(12):2721–2751

Prentice IC et al (2001) The carbon cycle and atmospheric carbon dioxide. In: Houghton JT et al (eds) Climate change 2001: the scientific basis. Cambridge University Press, New York

Qian T, Dai A, Trenberth KE, Oleson KW (2006) Simulation of global land surface conditions from 1948 to 2004. Part I: forcing data and evaluations. J Hydrometeorol 7:953–975

Randerson JT et al (2009) Systematic assessment of terrestrial biogeochemistry in coupled climate-carbon models. Glob Change Biol 15(10):2462–2484

Schimel D et al (1995) CO_2 and the carbon cycle. In: Houghton JT et al (eds) Climate change 1994, radiative forcing of climate change and evaluation of the IPCC IS92 emission scenarios. Cambridge University Press, New York

Schuur EAG et al (2008) Vulnerability of permafrost carbon to climate change: implications for the global carbon cycle. Bioscience 58(8):701–714

Schuur EAG et al (2009) The effect of permafrost thaw on old carbon release and net carbon exchange from tundra. Nature 459(7246):556–559

Sellers PJ et al (1996) Comparison of radiative and physiological effects of doubled atmospheric CO_2 on climate. Science 271(5254):1402–1406

Sitch S et al (2008) Evaluation of the terrestrial carbon cycle, future plant geography and climate-carbon cycle feedbacks using five Dynamic Global Vegetation Models (DGVMs). Glob Change Biol 14(9):2015–2039

Thompson SL et al (2004) Quantifying the effects of CO_2-fertilized vegetation on future global climate and carbon dynamics. Geophys Res Lett 31(23):L23211. doi:10.1029/2004GL021239

Thornton PE, Lamarque JF, Rosenbloom NA, Mahowald NM (2007) Influence of carbon-nitrogen cycle coupling on land model response to CO(2) fertilization and climate variability. Glob Biogeochem Cycles 21:GB4018. doi:10.1029/2006GB002868

Thornton PE et al (2009) Carbon-nitrogen interactions regulate climate-carbon cycle feedbacks: results from an atmosphere-ocean general circulation model. Biogeosciences 6(10):2099–2120

Zaehle S, Friedlingstein P, Friend AD (2010) Terrestrial nitrogen feedbacks may accelerate future climate change. Geophys Res Lett 37:L01401. doi:10.1029/2009GL041345

Zeng N, Qian HF, Munoz E, Iacono R (2004) How strong is carbon cycle-climate feedback under global warming? Geophys Res Lett 31:L20203. doi:10.1029/2004GL020904

Zickfeld K, Eby M, Matthews HD, Schmittner A, Weaver AJ (2011) Nonlinearity of carbon cycle feedbacks. J Clim 24(16):4255–4275

Zwiers F, von Storch H (1995) Taking serial correlation into account in tests of the mean. J Clim 8:336–351